Tetrahedron 65 (2009) 4356–4366

Contents lists available at ScienceDirect

Tetrahedron

journal homepage: www.elsevier.com/locate/tet

Synthesis and conformational analysis of glycomimetic analogs of thiochitobiose

Anja Fettke, Dirk Peikow, Martin G. Peter, Erich Kleinpeter *

Chemisches Institut, Universität Potsdam, Karl-Liebknecht-Straße 24-25, D-14476 Potsdam (Golm), Germany

ARTICLE INFO

Article history:
Received 18 February 2009
Received in revised form 20 March 2009
Accepted 23 March 2009
Available online 1 April 2009

Keywords:
Carbohydrates
S-Glycosides
Thiochitobiose
Conformational analysis
Molecular modeling
^{1}H NMR spectroscopy
NOE

ABSTRACT

The synthesis of six analogs of *N*,*N*′-diacetylchitobiose is reported, including a novel transglycosylation reaction for the preparation of *S*-aryl thioglycosides. The conformations of the compounds were studied by a combination of NMR spectroscopy and molecular modeling, using force field calculations. In the case of the *S*-aryl thioglycosides with exclusively *S*-glycosidic linkages, dihedral angles of the disaccharidic *S*-glycosidic bonds, Φ' and Ψ' and of the *S*-arylglycoside bonds, Φ and Ψ, were found to be similar, whereas they were different in mixed glycosides and in a thiazoline derivative. An adequate correlation between the calculated H,H-distances of the local minima and the measured NOE contacts was achieved by applying population-weighted averages over participating conformers based on weighted relative energies.

1. Introduction

Oligosaccharides composed of β-(1,4)-linked *N*-acetylglucosamine, so called chitooligosaccharides, are formed in nature by enzymatic degradation of chitin. Increasing evidence indicates that these compounds function as signaling molecules in some fundamental biological processes, such as pattern formation in vertebrates[1] and synthesis of hyaluronic acid (for reviews, see Refs. 2 and 3). In this context, the enzymes involved in the formation of chitooligosaccharides are studied intensively.[4–8] Within our work on the mechanism and inhibition of chitinases,[9–18] we report here on the synthesis and conformation of four novel O- and S-glycosides of *N*,*N*′-diacetylthiochitobiose **2**–**5**, respectively, as well as the known analog **1**.[19] As sulfur is less basic than oxygen, S-glycosides with respect to the *O*-analogs would be more resistant to acid catalyzed enzymatic hydrolysis[20–26] and thus may represent competitive chitinase and/or hexosaminidase inhibitors. In addition, we have prepared the thiazoline derivative **6**, which mimics the corresponding oxazoline derivative that occurs as an intermediate during the hydrolysis of chitin by family 18 glycosyl hydrolases,[27] including also chitinases and *N*-acetylhexosaminidases. Thus, as an analog of the intermediate,[28–32] **6** could act as an inhibitor of family 18 chitinolytic enzymes.

The conformational behavior of compounds **1**–**6** (Scheme 1) has been investigated by the combination of NMR spectroscopy and molecular modeling, using force field calculations. On the one hand the NMR spectroscopy is the method of choice for assessing the conformation of oligosaccharides in aqueous solutions as well as in the protein bound state.[33] But on the other hand the limiting problem in determining the solution state conformation is that oligosaccharides populate several conformations at ambient temperature[34] with respect to the glycosidic linkages. As a consequence of this limitation, H,H-coupling constants and NOE enhancements prove to be weighted averages of this unknown number of conformers. In order to accompany and support the experimental conformational NMR study, computational methods have to be incorporated. Especially force field methods afforded useful and widely suitable results; hence the oligosaccharides **1**–**6** (Scheme 1) were studied by molecular mechanical calculations using the AMBER force field. Internuclei distances in the conformers, that participates in the conformational equilibria were examined and compared with the experimental NOEs. Because of the disagreement of the experimental NMR data and the theoretically obtained global minimum structure, several conformations had to be considered as *Boltzmann* population-weighted averages subject to their relative energies.

2. Results and discussion

2.1. Synthesis

Conversion of 2-acetamido-3,4,6-tri-*O*-acetyl-2-deoxy-α-D-glucopyranosyl chloride (**7**) or pentaacetylglucosamine (**8**) to methyl glucosaminide **9**[19] and the corresponding *p*-methoxyphenyl

* Corresponding author. Tel.: +49 331 977 5210; fax: +49 331 977 5064.
E-mail address: kp@chem.uni-potsdam.de (E. Kleinpeter).

0040-4020/$ – see front matter © 2009 Elsevier Ltd. All rights reserved.
doi:10.1016/j.tet.2009.03.067

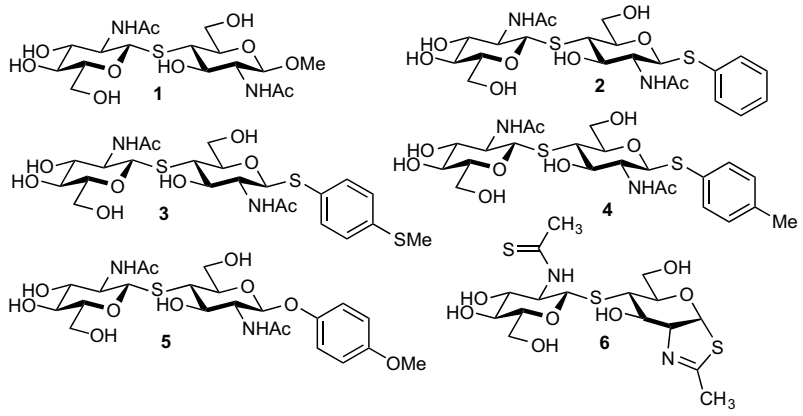

Scheme 1. Structures of studied compounds.

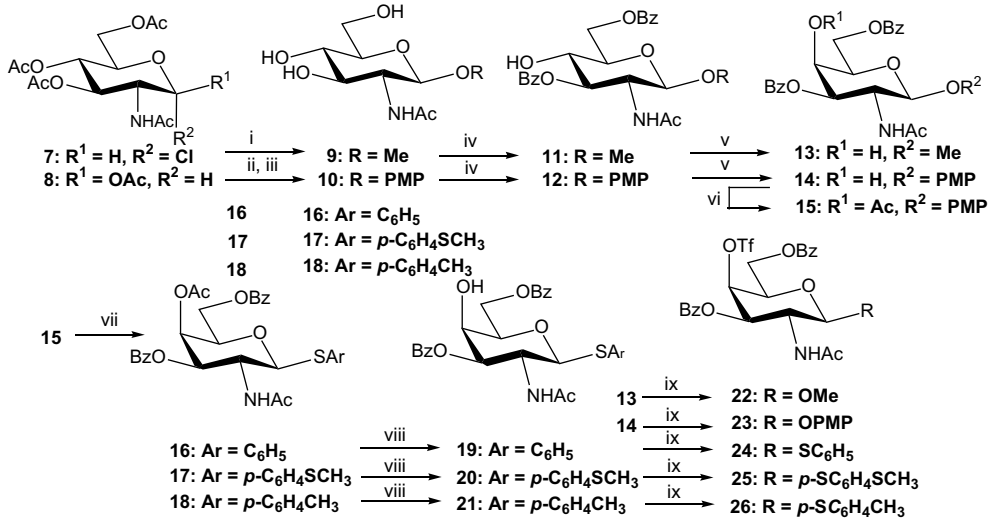

Scheme 2. Synthesis of 4-*O*-Tf-galactoside acceptors. (i): NaOMe, MeOH, CH_2Cl_2, rt, 2 h (76%); (ii): *p*-methoxyphenol, $BF_3{\cdot}Et_2O$, CH_2Cl_2, rt, 72 h (87%); (iii): LiOH, MeOH, rt, 4–8 h (94%); (iv): BzCl, Py, −60 °C→rt, 16 h (**11**: 87%; **12**: 78%); (v): Tf_2O, Py, CH_2Cl_2, −15 °C, 1 h, then $NaNO_2$, DMF, rt, 16 h (**13**: 86%, **14**: 58%); (vi): Ac_2O, Py, 0 °C→rt, 24 h (96%); (vii): aryl-SH, $BF_3{\cdot}Et_2O$, molecular sieves 4 Å, $CHCl_3$, 60 °C, 24 h (**16**: 79%, **17**: 68%, **18**: 67%);(viii): AcCl, MeOH, $CHCl_3$, 0 °C→rt, 24–48 h (**19**: 56%, **20**: 54%, **21**: 17%); (ix): Tf_2O, Py, CH_2Cl_2, 0 °C, 2 h (**22**: 99%, **23**: 99%, **24**: 99%, **25**: 99%, **26**: 99%).

glycoside **10**,[35,36] respectively, was carried out by standard procedures (Scheme 2). Regioselective benzoylation of **9** and **10** afforded the 3,6-di-*O*-benzoyates **11** and **12**, respectively, which were epimerized[19] to the corresponding galactosaminides **13** and **14**. Acetylation of **14** afforded the 4-*O*-acetate **15**. The S-glycosides **16**, **17**, and **18** were obtained from **15** by a novel transglycosylation with appropriate arylthiols in the presence of $BF_3{\cdot}OEt_2$. Selective 4-O-deacetylation of **16**–**18** gave the 4-OH galactosides **19**–**21**, respectively. The 4-*O*-trifluoromethanesulfonyl acceptors **22**–**26** were prepared by 4-O-sulfonylation of *galacto* acceptors **13**, **14**, and **19**–**21**, respectively, in nearly quantitative yield.

Coupling of the acceptors with the thio donor **27**[37,38] in the presence of NaH and 15-crown-5 (cf. Ref. 19) afforded the corresponding protected *N*,*N*′-diacetylthiochitobiosides **28**–**32** (Scheme 3). Finally, *Zemplen* cleavage[39] of the *O*-acetyl and *O*-benzoyl groups gave the free pseudotrisaccharides **1**–**3**, **5**, and **6** in excellent yields. Thionation of **32** with *Lawesson* reagent[40,41] afforded, instead of the expected bis-thioacetamide, the mono-thioacetamidoglucosyl α-*gluco*-tetrahydropyranothiazoline **33**, which was deprotected under *Zemplen* conditions to give the free pseudo-disaccharide **4** (Scheme 3).

The structures of **1**–**6** were confirmed by ^1H and ^{13}C NMR spectroscopy, employing COSY, TOCSY, NOESY, HMQC, and HMBC experiments. Anomeric protons were useful entry points into analysis of spin systems. From the HMBC spectra both quaternary carbons and interresidue connectivities, could be unequivocally assigned by examining the H-1′, C-4 cross-peaks (Scheme 4); ^1H, ^{13}C chemical shifts and vicinal coupling constants between H-1 and H-2, H-5 and H-6*proS*, and H-5 and H-6*proR*, respectively, for compounds **1**–**6** are given in Tables 1 and 2. Due to the lower electronegativity of sulfur, the coupling constants $^3J_{H1'-H2'}$ of the trans diaxial protons of the *S*-glycosidic nonreducing end GlcNAc residues were ca. 10.5 Hz, which is 1–2 Hz higher than in the corresponding chitooligosaccharides possessing *O*-glycosidic linkages.[10,13,42]

In the reducing end GlcNAc units, the corresponding values $^3J_{H1-H2}$ were 7.0–10.5 Hz, dependent on the nature of the glycosidic atom (Table 1). The small $^3J_{H1-H2}$ value of 7.0 Hz in the thiazoline residue is consistent with the cis pseudo equatorial orientation of H-1 and H-2 in the five-membered heterocyclic ring, confirmed by the NOE enhancement between H-1 and H-2.

2.2. Conformational analysis

The detailed assignment of both ^1H and ^{13}C spectra is based on NOESY measurements by examining inter- and intraresidual NOEs.

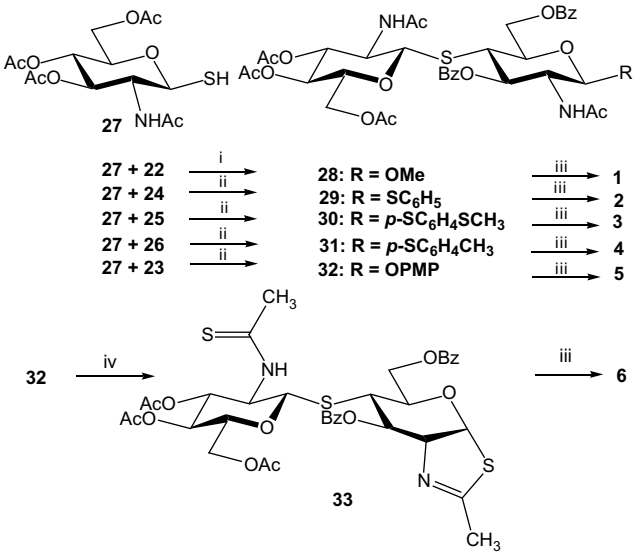

Scheme 3. Synthesis of thiochitobiose derivatives. (i): NaH, DMF, 0 °C→rt, 5–16 h (57%); (ii): NaH, 15-crown-5, THF, rt, 6 h (**28**: 57%, **29**: 31%, **30**: 28%, **31**: 33%, **32**: 47%); (iii): NaOMe, MeOH, rt, 16 h (87–97%); (iv): *Lawesson* reagent, toluene, 80 °C, 72 h (56%).

Therefore compounds **1**–**6** were subjected to 2D-NOESY experiments using a general mixing time of 500 ms, which was applied in all NOESY-experiments (at this mixing time, tentative intensity build up curves proved NOEs to attain maximal values). Under these conditions, distances r_{ij} between the corresponding protons were calculated from a known distance r_{kl} by using the accepted relationship $r_{ij}=r_{kl}(\sigma_{kl}/\sigma_{ij})^{1/6}$ (σ_{ij} and σ_{kl} are cross-relaxation rates between protons i and j and between protons k and l, respectively).[43] It was not attempted to calculate precise distances because of severe signal overlap and the uncertainty in the dynamic properties of carbohydrate and heterocyclic parts of the compounds. Only upper and lower limits of interproton distances were estimated by calibration against the known distances between two adjacent aromatic protons (e.g., H-10 and H-11; 2.48±0.01 Å) in **2**–**5** or between H-1 and H-5 of the pyranose ring (2.24±0.01 Å) in **1** and **6** of the nonreducing residue of *N*-acetylglucosamine. The intensities of the NOE cross-peaks in NOESY spectra were determined and compared to the intensities of the NOEs between H-10 and H-11 and H-1 and H-5, respectively, and assessed as *very strong* ($d_{H,H}$<2.8 Å), *strong* (2.8 Å<$d_{H,H}$<3.2 Å), *medium* (3.2 Å<$d_{H,H}$<3.6 Å), and *weak* (3.6 Å<$d_{H,H}$<4.0 Å).[10,13]

As further NMR parameters, to determine solution conformations, both homonuclear H,H and heteronuclear H,C coupling constants, in particular the trans-glycosidic $^{1}H-^{13}C$ *J*-coupling constant, could be potentially employed. However, because of the very low quantity of compounds **1**–**6** only the $^{3}J_{H,H}$-couplings in terms of CH_2OH rotamers could be consulted.

Since the NOEs determined represent the population-weighted averages of the NOEs of all conformers participating in the conformational equilibrium, NMR data alone can rarely define the conformational composition of oligosaccharides unambiguously.

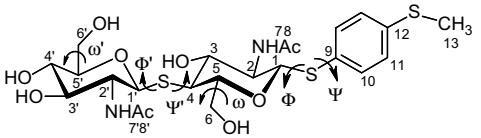

Scheme 4. Denomination of atoms, bonds, and torsional angles.

Table 1
^{1}H chemical shifts (δ/ppm) and the vicinal H1–H2 and H5–H6 coupling constants (Hz) of compounds **1**–**6** [D_2O]

	Monomer	1,1′	2,2′	3,3′	4,4′	5,5′	6*R*/*S*,6′*R*/*S*	8,8′ (NHAc)	10	11	12/13 (Me)	$^{3}J_{H1-H2}$	$^{3}J_{H5-H6pS}$	$^{3}J_{H5-H6pR}$
1	GlcNAc-O-Me	4.42	3.63–3.68	3.54–3.61	2.88	3.63–3.68	3.87–3.92/4.10	2.04			3.50	8.5	2.1	5.5
	GlcNAc′-S-	4.72	3.70–3.75	3.54–3.61	3.46–3.48	3.46–3.48	3.70–3.75/3.87–3.92	2.05				10.5	2.2	5.6
2	GlcNAc-S-arom.	4.91	3.80	3.63	2.95	3.69–3.75	3.88–3.91/4.06	2.04	7.53	7.37–7.43	7.37–7.43	10.4	2.1	5.3
	GlcNAc′-S-	4.73	3.69–3.75	3.58	3.46–3.47	3.46–3.47	3.69–3.75/3.88–3.91	2.04				10.5	1.8	5.6
3	GlcNAc-S-arom.	4.67	3.45–3.53	3.43	2.68	3.45–3.53	3.64–3.68/3.82	1.85	7.14	7.29	2.35	10.4	2.0	5.1
	GlcNAc′-S-[b]	4.57	3.45–3.53	3.30	3.16	3.20–3.23	3.45–3.53/3.64–3.68					10.6	2.3	5.9
4	GlcNAc-S-arom.	4.80	3.73	3.52–3.67	2.82	3.52–3.67	3.77–3.82/3.95	1.99	7.37	7.22	2.33	10.4	2.0	5.0
	GlcNAc′-S-[b]	4.65	3.52–3.67	3.44	3.27–3.31	3.34–3.37	3.52–3.67/3.77–3.82	1.97				10.6	2.1	5.8
5	GlcNAc-O-arom.	5.02	3.91–3.96	3.69	2.99	3.73–3.77	3.91–3.96/4.09	2.04	7.04	6.97	3.81	8.6	2.2	4.8
	GlcNAc′-S-	4.75	3.73–3.77	3.59	3.48–3.49	3.48–3.49	3.73–3.77/3.91–3.96	2.06				10.4	2.1	5.6
6	NAG-Thiazoiln	6.33	4.49	4.74–4.82	2.94	3.36	3.59/3.80	2.26				7.0	2.3	6.8
	GlcNAc′[a]-S-	4.74–4.82	4.66	3.65	3.49–3.52	3.49–3.52	3.73/3.92	2.52[a]				10.5	2.0	5.8

[a] C=S, estimated error for $^{3}J_{5,6}$=±0.2 Hz.
[b] D_2O/DMSO.

Table 2
^{13}C chemical shifts (δ/ppm) of compounds **1–6** [D_2O]

	Monomer	1,1′	2,2′	3,3′	4,4′	5,5′	6*R*/*S*,6′*R*/*S*	7,7′ (C=O/*S*)	8,8′ (NHAc)	9	10	11	12	13 (Me)
1	GlcNAc-*O*-Me	106.8	61.9	76.6	53.3	91.5	66.5	179.7	27.1					62.1
	GlcNAc′-*S*-	88.9	60.0	79.9	74.7	84.9	65.8	179.7	27.3					
2	GlcNAc-*S*-arom.	90.7	60.2	76.9	52.4	85.0	66.0	178.8	26.6	136.6	136.0	133.8	132.6	
	GlcNAc′-*S*-	88.1	59.4	79.3	74.1	84.3	65.2	179.0	26.6					
3	GlcNAc-*S*-arom.	87.1	56.7	73.2	49.0	81.7	62.7	173.7	23.7/23.8	130.5	127.8	132.7	139.0	15.7
	GlcNAc′-*S*-	84.2	56.0	76.1	71.1	81.3	62.2	173.9	23.7/23.8					
4	GlcNAc-*S*-arom.	87.3	56.7	73.2	49.0	81.6	62.6	173.4	23.7	130.8	131.9	131.2	138.7	21.7
	GlcNAc′-*S*-	84.2	56.0	76.1	71.1	81.2	62.1	173.7	23.7					
5	GlcNAc-*O*-arom.	104.8	61.3	75.6	52.4	81.1	65.7	179.3	26.6	155.5	122.8	119.5	159.3	60.3
	GlcNAc′-*S*-	88.3	59.4	79.3	74.1	84.3	65.2	179.0	26.6					
6	NAG-Thiazoiln	92.3	82.0	76.6	50.3	77.9	66.6	176.6	23.8					
	GlcNAc[a]-*S*-	90.0	64.8	79.8	74.0	84.5	65.3	208.7[a]	37.2[a]					

[a] C=*S*.

Therefore, the conformational analysis of these highly flexible oligosaccharides requires additional assistance of molecular modeling to acquire conformational information. For this reason, population-weighted average distances were calculated considering the conformers of **1**–**6** and were compared to the experimentally observed NOE data at room temperature. Temperature dependency of the equilibria was not studied.

Even though the AMBER force field described by Woods et al.[44] has fully compatible parameters for common carbohydrates, parameters involving the *S*-glycosidic linkage and the thioacetamide moiety are not included. Hence, the AMBER99-GLYCAM04 parameter set had to be completed for the studied compounds **1**–**6** and the monomer database, included in the SYBYL program package (vide infra) was accumulated with the new carbohydrate and aromatic monomers (see also Experimental section). In Figure 1, the torsional angle of the *S*-glycosidic linkage (O–C^1–*S*–C^4), obtained by the modified AMBER force field, has been compared with the result of the ab initio calculation. Excellent results were obtained and the thus freshly paramerized force field was employed for the grid search calculations of **1**–**6**.

Each molecule was exposed to an extensive systematic conformational search. Grid search simulations in 10° increments from 0 to 350° were run to calculate relaxed potential energy (Φ/Ψ, Φ'/Ψ') maps with the expanded modified AMBER force field. The torsional angles at the glycosidic linkages are commonly defined as: Φ (H1′–C1′–*S*–C4) and Ψ (C1′–*S*–C4–H4) for **1** and **6**; Φ' (H1′–C1′–*S*–C4) and Ψ' (C1′–*S*–C4–H4) for **2**–**5**; and Φ (H1–C1–*X*–C9) and Ψ (C1–*X*–C9–C10) for **2**–**5** with *X*=*O* or *S* (Scheme 4).

Population-weighted averages were then calculated from the global and local conformational minima, thus obtained, employing weighting factors based on *Boltzmann* distributions,[45] which were calculated from the relative energies. The experimentally observed interresidue H,H-distances, which characterize the conformation of the sugar-sugar-(pyranosyl)-glycosidic linkage of compounds **1**–**6** are displayed in Table 3 together with the calculated H,H-distances of the minimum states A–D and the population-weighted internuclear proton–proton distances of all conformational minima, the minimum states A and the sum of minimum states A and B, respectively.

The accurate determination of the NOEs in D_2O was limited due to existing signal overlap. The observed interglycosidic NOEs measured at ambient temperature indicate at least for compounds **2** and **5** more than one solution conformation. The other compounds reveal strong signal overlap in the regions of interglycosidic NOEs. The presence of the H1′–H3 NOE in **2** and **5** indicates that the

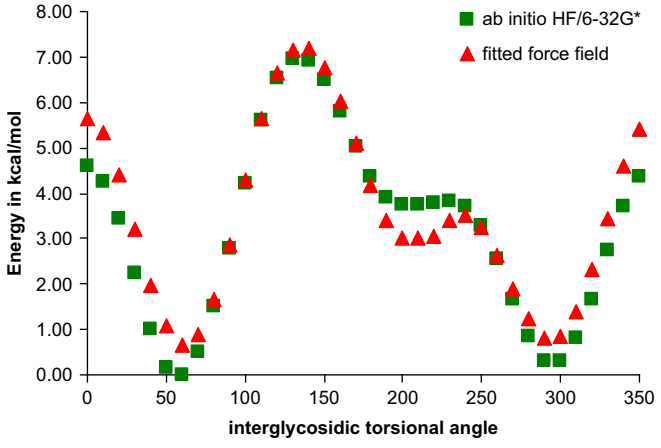

Figure 1. Comparison of ab initio and force field calculated interglycosidic torsional angle (O–C^1–*S*–C^4).

Table 3
Comparison of intensities of Φ'/Ψ'-interresidual NOEs from experimental NOESY spectra with internuclear distances for low-energy conformers of **1**–**6** as obtained from force field calculations together with population-weighted average values

	H–H	Theoretical distances respecting Φ'/Ψ'				Obsd signal-intensity	p-w average distance [Å] overall conf.	p-w average distance [Å] over A	p-w average distance [Å] over A+B
		A	B	C	D				
1	H1′–H4	4.6	3.8	2.3	3.9	w	3.9	4.6	4.3
	H1′–H3	3.8	5.1	4.7	2.1	overlaid	4.0	3.8	4.2
	H1′–H5	4.3	5.1	4.2	3.7	n.d.	4.4	4.3	4.5
	H1′–H6*pR*	4.4	3.9	2.9	4.7	w	4.1	4.4	4.2
	H1′–H6*pS*	5.9	5.7	4.3	5.8	n.d.	5.6	5.9	5.8
	H1–OMe	2.7	2.7	2.8	2.7	vs	2.7	2.7	2.7
2	H1′–H4	3.8	2.3	4.6	3.9	s	3.4	3.7	3.2
	H1′–H3	5.1	4.7	3.9	2.1	w	4.7	5.1	5.0
	H1′–H5	5.1	4.3	4.4	3.6	w	4.7	5.1	4.8
	H1′–H6*pR*	3.9	2.9	4.4	4.7	w	3.7	3.9	3.6
	H1′–H6*pS*	5.6	4.2	5.9	5.7	n.d.	5.2	5.6	5.1
	H1–HoPhen	4.5	4.5	4.4	4.4	m	4.5	4.5	4.5
3	H1′–H4	3.8	2.3	3.9	4.6	s	3.3	3.8	3.2
	H1′–H3	5.1	4.7	2.1	3.9	w-m	4.6	5.2	5.1
	H1′–H5	5.1	4.2	3.6	4.3	w	4.6	5.2	4.8
	H1′–H6*pR*	3.9	2.9	4.7	4.3	w	3.6	3.9	3.5
	H1′–H6*pS*	5.6	4.2	5.7	5.9	n.d.	5.1	5.7	5.1
	H1–HoPhen	4.5	4.5	4.4	4.4	n.d.	4.5	4.5	4.6
4	H1′–H4	3.8	2.3	3.9	4.6	m-s	3.3	3.8	3.1
	H1′–H3	5.1	4.7	2.1	3.9	w-m	4.6	5.2	5.0
	H1′–H5	5.1	4.3	3.6	4.3	n.d.	4.5	5.2	4.7
	H1′–H6*pR*	3.9	3.0	4.7	4.4	n.d.	3.7	3.9	3.5
	H1′–H6*pS*	5.6	4.3	5.7	5.9	w	5.1	5.7	5.0
	H1–HoPhen	4.5	4.5	4.4	4.4	n.d.	4.5	4.5	4.5
5	H1′–H4	4.6	3.8	3.9	2.3	w	4.0	4.5	4.2
	H1′–H3	3.8	5.1	2.1	4.7	w	4.0	3.7	4.2
	H1′–H5	4.3	5.1	3.7	4.2	w	4.4	4.2	4.5
	H1′–H6*pR*	4.4	3.9	4.7	2.9	w	4.1	4.2	4.1
	H1′–H6*pS*	5.9	5.6	5.8	4.2	n.d.	5.6	5.7	5.6
	H1–HoPhen	3.3	3.4	3.3	3.3	s	3.4	3.2	3.3
6	H1′–H4	2.3	3.7	3.8	4.6	s	3.2	2.3	2.9
	H1′–H3	4.7	5.2	2.1	3.9	n.d.	4.3	4.7	4.9
	H1′–H5	4.2	5.0	2.6	4.3	w	4.1	4.0	4.4
	H1′–H6*pR*	3.1	4.7	5.1	5.9	n.d.	4.2	3.0	3.7
	H1′–H6*pS*	2.5	3.8	4.1	4.5	w	3.3	2.4	3.0

synΦ/*antiΨ* minimum is heavily populated while the presence of the H1′–H4 NOE as well as the H1′-H-6*proR/S*-NOEs in **1**–**6** indicate the presence of the *synΦ*/*synΨ* conformer. The H2′-H5 and the H2′-H3 NOE can theoretically describe the *antiΦ*/*antiΨ* conformation whereas the H2′-H4 NOE describes the *antiΦ*/*synΨ* conformation. Due to the strong signal overlap of the ring protons and the vicinity of the potential H2′-H5/H2′-H3 NOEs to the peaks of the diagonal it was difficult to conclude whether the *antiΦ*/*synΨ* or the *antiΦ*/*antiΨ* conformation were present.

The population-weighted averaged H,H-distances from the force field, given in Table 3, are in sufficient agreement with experimentally obtained H,H-distances in terms of obtained NOE enhancements. The agreement is already good if conformations A and B were taken into account, in **1** both conformers contribute 71% (A: 49%), in **2** 84% (A: 54%), in **3** 84% (A: 44%), in **4** 82% (A: 44%), in **5** 74% (A: 46%), and in **6** 72% (A: 43%) to the overall population. Consideration of all conformational minima reveals similar values as for A+B only due to their high contributions. The averaged H,H-distances of A+B for the Φ'/Ψ'-interglycosidic linkages correspond to two different conformers for **1** and **6**, to 12 different conformers for **2**–**4** and to 8 different conformers for **5**, since with increasing glycosidic linkages the number of potential solution conformations increases as well.

Both the experimental and calculated H,H-distances, given in Table 3, show clearly the differences between the compounds with exclusively *S*-glycosidic linkages (**2**–**4**, **6**), which exhibit predominantly strong H1′–H4 NOEs, and the compounds with mixed glycosidic linkages (**1** and **5**), which exhibit only weak H1′–H4 NOEs. Thus, the type of the adjacent glycosidic linkage proves to be of considerable conformational influence.

Another conformational flexibility of oligosaccharides exists for the conformation of the exocyclic hydroxymethyl group. In this work, only gg and gt orientations had to be taken into account; the population of the tg conformer is low because the vicinal coupling constants of H-5 and H-6*proS* and H-5 and H-6*proR*, respectively, in **1**–**6** show a rotameric distribution that tends to gg≥gt≫tg as concluded from the experimental values by employing Eqs. I–III in Table 4.[46–49] These results are in accordance with studies on other glucosaminides,[10,13] e.g., by Nishida et al.,[50] who found the rotameric distribution of *N*-acetylglucosamine in aqueous solution to be gg:gt:tg≈60:40:0; thus, four combinations for the disaccharide units were considered exemplary (gg–gg, gg–gt, gt–gg, gt–gt). It was found that the shape of the potential energy surface was independent of the initial conformation of the hydroxymethyl group as reported previously.[51] Therefore, we used subsequently the hydroxymethyl group orientations ω and ω' as calculated from the vicinal coupling constants of H-5/H-6*proS*/*proR*; they are given in Table 4.

For all calculations, a distance-dependent dielectric constant of 78 was used to implicitly consider the presence of water as solvent because of the strong tendency of carbohydrates to form inter- and intramolecular hydrogen bonds.

Table 4
Determination of rotameric distributions of the CH_2OH group in **1–6** [D_2O] employing Eqs. I–III[45–48]

I 1.3gg + 2.7gt + 11.7tg = $J_{H5\text{-}H6proS}$
II 1.3gg + 11.5gt + 5.8tg = $J_{H5\text{-}H6proR}$
III gg + gt + tg = 1

Monomer	Hz		Rotameric distribution in %		
	$^3J_{H5-H6pS}$	$^3J_{H5-H6pR}$	gg	gt	tg
1 GlcNAc-OMe	2.1	5.5	57	40	3
GlcNAc′	2.2	5.6	57	40	3
2 GlcNAc-*S*-Phenyl	2.1	5.3	60	37	3
GlcNAc′	1.8	5.6	58	42	0
3 GlcNAc-*S*-Phenyl-SMe	2.0	5.1	62	36	2
GlcNAc′	2.3	5.9	53	43	4
4 GlcNAc-*S*-Phenyl-Me	2.0	5.0	63	35	2
GlcNAc′	2.1	5.8	56	43	1
5 GlcNAc-*O*-Phenyl-OMe	2.2	4.8	63	32	5
GlcNAc′	2.1	5.6	56	41	3
6 NAG-Thiazolin	2.3	6.8	44	52	4
GlcNAc(S)′	2.0	5.8	54	42	4

The torsional angles between the β-(1′-4)-*S*-glycosidic linkages and the β-(1-9)-*S*- and β-(1-9)-*O*-arylglycosidic linkages, respectively, and the aromatic moiety strongly influence the dynamic conformational space of compounds **1**–**6**. Figure 2 displays the conformational maps of the *S*-glycosidic intersugar Φ/Ψ or Φ'/Ψ' linkage, respectively, in these compounds. Conformational maps of the β-(1-9)-*S*- and β-(1-9)-*O*-arylglycosidic Φ/Ψ linkages between the middle sugar residue and the aromatic moiety in **2**–**5** are displayed in Figure 4 and will be discussed subsequently.

For the *S*-pyranosylglycosidic linkages between two sugar residues four local minimum conformer families were obtained (Fig. 2). The minimum conformation and the corresponding population distribution, proved to be similar to those reported for *N*,*N*′-diacetyl-4-thiochitobiose by Munoz et al.,[52] using the AMBER force field as well. Three main minimum conformations were found for the reducing end 4-thio-GlcNAc residue (A: 58/192, B: 52/13, C: 173/1). For compound **1**, the closest analog to *N*,*N*′-diacetyl-4-thiochitobiose, very similar minimum conformations A–C and, additionally the *anti*Φ/*anti*Ψ conformer as global minimum were obtained while for the three structurally similar compounds **2**–**4** the conformational maps proved to be nearly identical; the global minimum conformation A is located around 170/5 for Φ'/Ψ' and 180/170 for Φ/Ψ (Table 5). Compared to **2**–**4**, the variation of the nonreducing sugar residue from GlcNAc to NAG-thiazoline in **6** influences the dihedral angles Φ and Ψ of the global minimum structure A. In contrast, the replace from *S*-aryl to the *O*-aryl in **5** influences Ψ but not Φ in the global minimum A compared to **2**–**4**.

The determination of the three-dimensional structures of S-glycosides and the comparison with those of O-glycosides is important for evaluating the *S*-isologs as prospective chitinase inhibitors. To determine the differences between the glycosidic isologs, we also investigated the potential energy surface for the analogs **1a** and **5a** where the *S*-pyranosylglycosidic linkages of **1** and **5** were replaced by *O*-pyranosylglycosidic linkages; similar results were obtained (Fig. 3). For the global minimum conformation of the β-(1-4)-*O*-pyranosylglycosidic linkage isologs Φ/Ψ values around 350/320 are reported.[10,13,53–56] Due to the structural difference of the pyranosylglycosidic linkage isologs (Table 6) the replace of the glycosidic linkage from *O*- to *S*-isologs increase distinctly the conformational flexibility and hence influences clearly but not drastically the whole energy surface and hence, the location of the global minimum, number of local minima, and their depth.

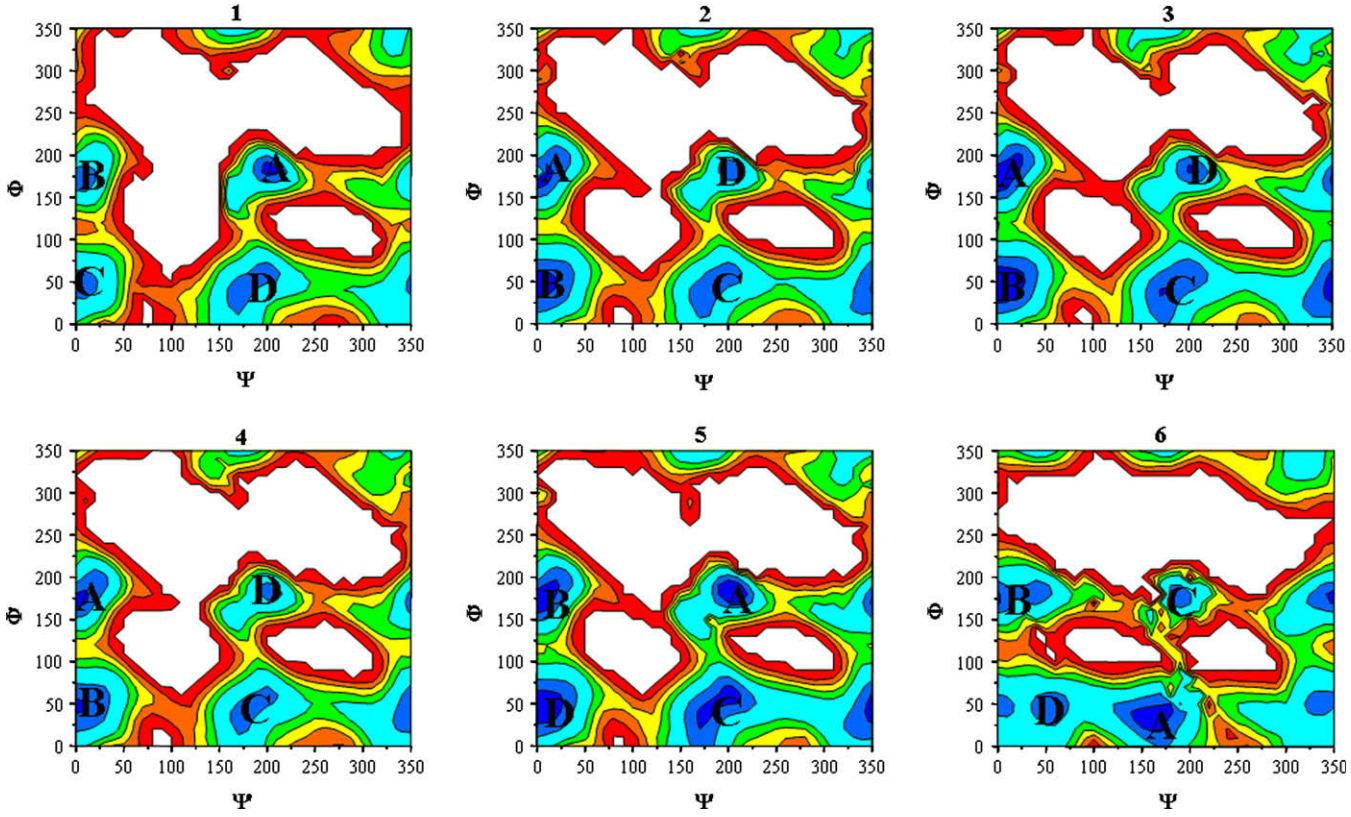

Figure 2. Contour plots for **1**–**6** concerning the interglycosidic torsional angles Φ and Ψ (**1**, **6**) or Φ' and Ψ' (**2**–**5**), respectively. Population densities are indicated by contour lines; A represents the global minimum, B–D are local minima.

Table 5
Torsional angles about glycosidic linkages and the corresponding relative energies of the conformational families of **1**–**6**

	Φ' and Ψ' (min)	Φ' and Ψ' (°)	Rel energy (kcal/mol)	Type of Φ' and Ψ'	Φ and Ψ (min)	Φ and Ψ (°)	Rel energy (kcal/mol)	Type of Φ and Ψ
1	—				A	183/204	0	*anti*/*anti*
	—				B	174/3	0.46	*anti*/*syn*
	—				C	49/4	0.62	*syn*/*syn*
	—				D	61/201	0.83	*syn*/*anti*
2	A	174/4	0	*anti*/*syn*	E	179/170	0.00–1.42	*anti*/*anti*
	B	48/5	0.35	*syn*/*syn*	E′	179/350	0.00–1.42	*anti*/*syn*
	C	59/199	1.25	*syn*/*anti*	F	57/178	0.90–2.11	*syn*/*anti*
	D	183/203	1.42	*anti*/*anti*	F′	57/357	0.90–2.11	*syn*/*syn*
					G	320/194	5.67–6.85	non-*exo*-*anti*
					G′	320/14	5.67–6.85	non-*exo*-*syn*
3	A	174/5	0	*anti*/*syn*	E	179/170	0.00–1.45	*anti*/*anti*
	B	49/3	0.07	*syn*/*syn*	E′	179/350	0.00–1.45	*anti*/*syn*
	C	58/199	0.84	*syn*/*anti*	F	57/177	0.92–2.03	*syn*/*anti*
	D	184/202	1.45	*anti*/*anti*	F′	57/357	0.92–2.03	*syn*/*syn*
					G	318/196	5.57–6.78	non-*exo*-*anti*
					G′	318/16	5.57–6.78	non-*exo*-*syn*
4	A	174/5	0	*anti*/*syn*	E	179/171	0.00–1.47	*anti*/*anti*
	B	49/3	0.06	*syn*/*syn*	E′	179/351	0.00–1.47	*anti*/*syn*
	C	58/199	0.85	*syn*/*anti*	F	57/178	0.92–2.03	*syn*/*anti*
	D	184/203	1.47	*anti*/*anti*	F′	57/357	0.92–2.03	*syn*/*syn*
					G	319/196	5.61–6.81	non-*exo*-*anti*
					G′	319/15	5.61–6.81	non-*exo*-*syn*
5	A	183/204	0	*anti*/*anti*	E	44/184	0.00–0.77	*syn*/*anti*
	B	174/3	0.28	*anti*/*syn*	E′	44/5	0.00–0.77	*syn*/*syn*
	C	61/202	0.62	*syn*/*anti*	F	192/120	2.06–2.67	*anti*/*anti*
	D	47/5	0.77	*syn*/*syn*	F′	192/298	2.06–2.67	*anti*/*syn*
6	—				A	31/154	0	*syn*/*anti*
	—				B	176/353	0.05	*anti*/*syn*
	—				C	178/188	0.44	*anti*/*anti*
	—				D	49/55	0.78	*syn*/*syn*

The conformational maps of **1a** and **5a** are very similar. In **1a** and **5a**, we found one low-energy conformation with dominating population and one additional energetically less stable conformer as found previously (Fig. S4 in Supplementary data).[10,13,53–56]

The global minima structures of **1a** and **5a** differ slightly concerning the Φ angle. Differences are caused only by the different aglycons on the disaccharidic residue. The global minimum of compounds **1a** and **5a** were found as local minimum B in **2**–**4**, as local minimum C in compound **1** and as local minimum D in compounds **5** and **6** in this work (Table 5). The minima concerning the *O*-arylglycosidic linkage in **5** are dominated by *exo*-anomeric conformations about *syn*Φ (like the minima A–C in **1a** and **5a**) as obtained similarly by Espinosa et al.[51] for the *N*-acetylglucosamine part and additionally by the crystal structure analysis of chitobiose;[56] the *S*-arylglycosidic linkage is however dominated by the *anti*Φ conformers.

Each of the disaccharidic *S*-pyranosylglycosidic low-energy conformers A–D, Φ' and Ψ', of **2**–**5** were set as starting point for the next run of grid search calculations about the dihedral angles, Φ and Ψ, of the *S*- or *O*-arylglycosidic bond, respectively. The conformational maps, thus obtained, for Φ and Ψ of **2**–**5** are displayed in Figure 4. For the *S*-arylglycosidic linkage in **2**–**4**, six local minimum conformer families were obtained, whereas for the *O*-arylglycosidic bond in **5**, four local minimum conformer families were obtained. As expected, the Φ/Ψ conformational maps of **5** and **5a** are similar both show low-energy-*syn*Φ-conformations (data for **5a** not shown). Because of the symmetry of the aromatic residue in **2**–**4** and **5**, the number of conformational families reduces to three and two, respectively.

For the three structurally analog compounds **2**–**4**, also the Φ/Ψ-conformational maps are very similar. The global minimum E/E′ is located at ca.180/170 and 180/350 (*anti*Φ). The local minima F/F′ are located at ca. 60/180 and 60/300 (*syn*Φ). In general, these positions of the local minima differ only slightly from the positions of the minima of the adjacent torsional angles Φ'/Ψ' (Table 5), but the potential energy surface as a whole varies clearly because of the structural difference between the sugar and aromatic residue, respectively. Furthermore, we found two additional and energetically equal minima G/G′ of higher energy (>5.5 kcal/mol) around 320/20 and 320/190 for **2**–**4**. Compared to **5** the contributions of which are less than 1% at 298 K and can hence be neglected. In **5** however the arylglycosidic global minimum E/E′ is located around 40/0 and 40/180 similar to the pyranosylglycosidic minima C and D of compound **5**. Thus, there is a clear but not drastic difference in the conformational maps between *S*- and *O*-arylglycosidic linkages concerning the location of the global minimum, number of local minima and their depth.

To sum up the grid search calculation results, four low-energy conformers were found for compounds **1** and **6**, 16 for compound **5**, and 24 (also 16 without the negligible G/G′-minima) for compounds **2**–**4** dependent on both the number of monomer entities and type of glycosidic linkage. The S-glycosides are conformationally more flexible in comparison to the O-glycosides and populate heavier the *anti*-conformations. The non-*exo*-*anti* and non-*exo*-*syn* minima are only minor populated and can be neglected.

A critical comparison of computed and experimentally determined H,H-distances in the global energy minimum conformer alone gives unsatisfying results (Table 3). If the NOEs, which result from internuclei distances averaged over the A and B conformers, are considered, they fit in with the experimental data. Although the distances between the interresidual protons are dominated by the global minimum, the fit is better, when also local minima are taken into account. This can be verified with the experimentally observed NOE contacts. The found NOEs between H-1′ and H-4 as well as the NOEs between H-1′ and H-6*proR*/*S*-NOEs indicate the existence of *syn*Φ/*syn*Ψ-conformers in solution and can be compared with

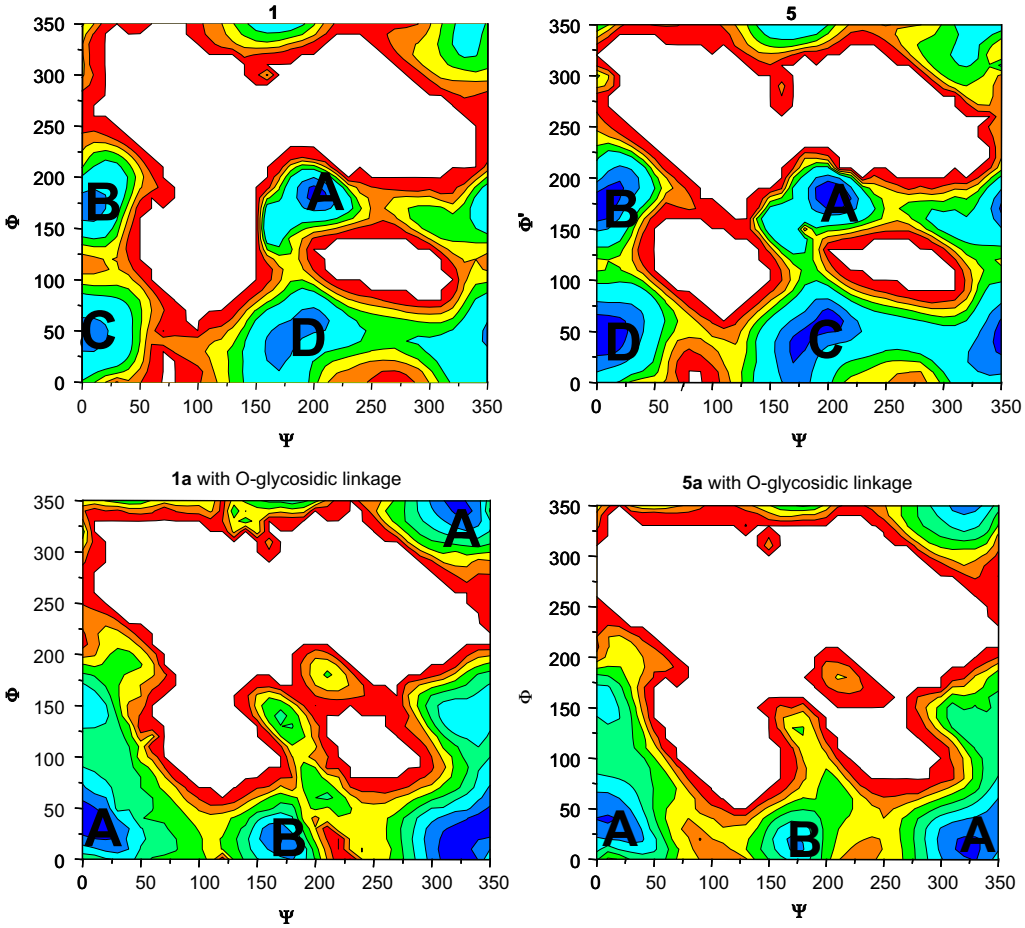

Figure 3. Comparison of *S*- and *O*-glycosidic linkages in **1** and **5** and in **1a** and **5a**, respectively (plots above represent *S*-glycosidic linkages, the plots below *O*-glycosidic linkages).

conformers B in **2**–**4** (Table 7), conformer C in **1** and conformers D in **5** and **6**. In addition the NOEs between H-1′ and H-3 militate in favor of high population of the *synΦ*/*antiΨ*-conformation and can be compared with conformers C in **2**–**5** (cf. in Table 7), conformer D in **1** and conformer A in **6**. Even though the conformational behavior in solution is dominated by up to eight (neglecting G/G′) conformers, there are still many other local minimum conformers of lower population that could slightly contribute to the averaged results. The eight dominating low-energy conformations of compound **2** are shown as examples in Table 7; all other conformations contribute less than 4%. The conformers concerning minimum A according to the disaccharidic linkage Φ'/Ψ', with ca. 170/5, are calculated to dominate the solution state with a population of more than 50%.

As mentioned above, the experimental and calculated H,H-distances given in Table 3 show clearly the differences between the compounds that have exclusively *S*-glycosidic linkages (**2**–**4**, **6**) and the compounds with mixed glycosidic linkages (**1** and **5**). We found that the type of an adjacent glycosidic linkage has an evident conformational influence. With regard to the conformational maps, this different NOE-behavior is caused by the different location of the global minimum conformers.

Table 6
Comparison of calculated C–X–C bond angles [°] and C–X distances [Å] for Φ'/Ψ' and Φ/Ψ in **5a**, **5**, and **3** with *X*=*O*, *S*

Angle/distance	**5a** (*O*′, *O*)	**5** (*S*′, *O*)	**3** (*S*′, *S*)
C4′–*X*–C1	114.63	103.03	102.50
C4–*X*–C9	123.30	123.20	118.70
C4′–*X*	1.42	1.82	1.82
X–C1	1.42	1.83	1.82
C4–*X*	1.42	1.42	1.81
X–C9	1.33	1.33	1.78

2.3. Enzymatic studies

The chitothiooligosaccharides **1**–**6** were investigated with respect to their ability as potential inhibitors of an insect cell line chitinase and a *N*-acetylhexosaminidase of *Chironomus tentans*, as well as with two bacterial chitinases, i.e., isoenzymes ChiA and ChiB from *Serratia marcescens* (for details, see Ref. 42). None of the compounds showed appreciable inhibition of the hydrolysis 4-methylumbelliferyl *N*,*N*′-diacetylchitobioside (GlcNAc$_2$-MU) by the insect chitinase and ChiA ($IC_{50}\geq$960 μM), while **2** and **6** where poor inhibitors of ChiB (IC_{50} 560 and 380 μM, respectively). The hydrolysis of GlcNAc-MU by the insect *N*-acetylhexosaminidase was inhibited by **2**, **3**, **4**, and **5** (IC_{50} 110–150 mM) while the IC_{50} of the inhibition of the hydrolysis of GalNAc-MU by this enzyme was 60 μM.

3. Conclusions

2D-NOESY NMR experiments and force field calculations show that the oligosaccharides studied adopt more than one conformation in aqueous solution. Congruent results were only reached by assessing population-weighted averaged conformers according to the *Boltzmann* function deduced from their calculated relative energies. These *S*-glycosidic oligosaccharides differ from the *O*-glycosidic isologs clearly but not drastically and hence, reflect the

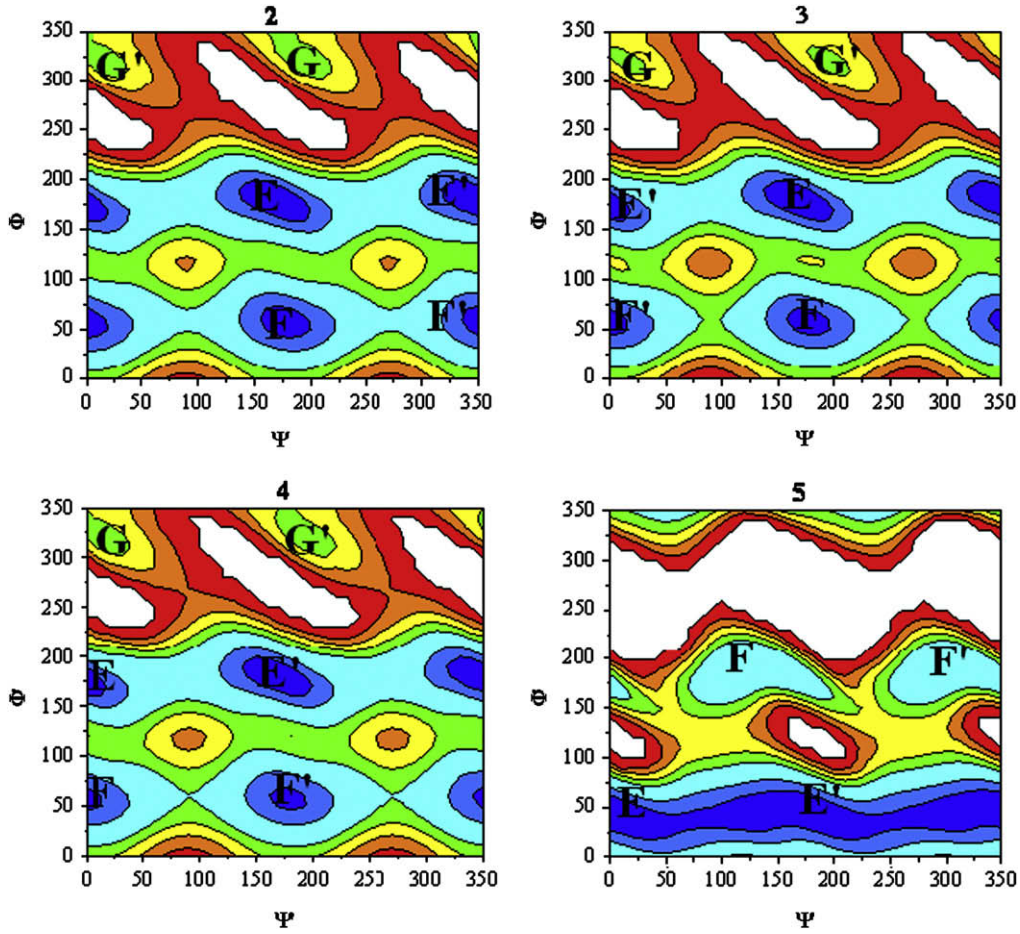

Figure 4. Contour plots for **2**–**5** with respect to torsional angles Φ and Ψ. Population densities are indicated by contour lines; E and E′ represent the global minimum concerning Φ and Ψ; F, F′ and G, G′ are other local minima.

higher conformational flexibility caused by the small energy barriers between the different regions of thiochito-oligosaccharidic conformational maps. Thus, minimum conformations different from the global minimum conformer may be bound to carbohydrate-active enzymes or sugar-binding proteins without eminent energy conflicts. This will be investigated in future with trNOESY and STD experiments.

Due to structural variations of the investigated pseudo-di- and trisaccharides **1**–**6**, we found that the type of glycosidic linkage, the replace of a sugar residue by an aromatic residue and the change from an *N*-acetylglucosamine to a NAG-thiazoline monomer induces changes of the conformational equilibria. These variations have only a slight influence on the location of the minima, but a clear influence on the potential energy surface affecting the location of the global minimum, the number of local minima and their depth. S-Glycosides are conformationally much more flexible than the *O*-isologs. Additionally, we found experimentally and theoretically that the conformation of a glycosidic linkage is evidently influenced by the type of the adjacent glycosidic linkage.

The enzyme assays show that compounds **2**–**5** reveal a low inhibition of the *N*-acetylhexosaminidase of *C. tentans* and of **2** and **6** of chitinase B of *S. marcescens*. These results lead to the conclusion that at least three monomer residues are necessary for a distinct inhibition, e.g., as the well known inhibitor allosamidine. Furthermore, an aromatic residue can take the place of a sugar unit but does not induce stronger inhibition, as compared with allosamidin; the same effect was found for the variation of the glycosidic linkage to a *S*-type analog. As the results of the molecular modeling calculations show, the change to the conformationally more flexible *S*-glycosidic linkage has no dramatically effect on the conformation but a distinct influence on the population. Thus, no decisive influence on the inhibition due to conformational differences can be expected, however, the effect of lower basicity of the *S*-glycosidic linkage should be considered.

Table 7
Torsional angles Φ,Ψ,Φ' and Ψ' of the eight preferred conformers of **2**; population in %

2 Conformer	C1′–*S*-C4 dihedral angle		C1–*S*–C9 dihedral angle		Population in %
	Φ'	Ψ'	Φ	Ψ	
1 (A/E)	172	3	179	350	22
2 (A/E′)	172	4	179	170	22
3 (B/E)	49	4	180	351	12
4 (B/E′)	49	4	179	170	12
5 (A/F)	174	4	58	357	5
6 (A/F′)	174	4	58	177	5
7 (C/E)	59	199	180	170	4
8 (C/E′)	59	199	180	350	4

4. Experimental section

4.1. Synthesis

Compounds **1**–**6** were obtained by de-O-acylation of **28**–**33**, respectively. The synthesis of **28**–**33** is described in Supplementary data, see also Ref. 42.

4.2. General procedure for de-O-acetylation and de-O-benzoylation of 28–33

The educt was added to a 0.4 M solution of NaOMe in MeOH, and the reaction mixture was stirred for 16 h at rt. Neutralization was followed by filtration, washing of the resin with MeOH, and concentration of the combined filtrate and washing solutions. The residue was suspended in H_2O and the mixture was freeze-dried.

*4.2.1. Methyl 2-acetamido-4-S-(2-acetamido-2-deoxy-β-D-glucopyranosyl)-2-deoxy-4-thio-β-D-glucopyranoside (**1**)*[19]

From **28** (503 mg, 0.38 mmol) in NaOMe/MeOH (20 mL). Colorless solid, yield: 160 mg (92%) [Ref.: 19 85%], mp 285.6 °C [Ref.: 19 200 °C], R_f=0.14 ($CHCl_3$/MeOH, 7:3). ^1H and ^{13}C NMR, see Tables 1 and 2. IR (KBr): ν=3271 (br ss), 2940 (m), 2863 (m), 1650 (ss), 1553 (ss), 1377 (s), 1315 (s), 1104 (br ss), 616 (s) cm^{-1}.

*4.2.2. Phenyl 2-acetamido-4-S-(2-acetamido-2-deoxy-β-D-glucopyranosyl)-2-deoxy-1,4-dithio-β-D-glucopyranoside (**2**)*

From **29** (78 mg, 0.09 mmol) in NaOMe/MeOH (10 mL). Colorless solid, yield: 46 mg (97%), mp 280 °C (decomp.), R_f=0.30 ($CHCl_3$/MeOH, 7:3). $[\alpha]_D^{27}$ −26 (*c* 0.3, DMSO). ^1H and ^{13}C NMR, see Tables 1 and 2. IR: ν=3386 (br ss), 2928 (s), 1654 (ss), 1553 (ss), 1374 (s), 1310 (s), 1056 (br ss), 610 (m) cm^{-1}. HR ESI MS: $C_{22}H_{33}N_2O_9S_2$, calcd $[M+H]^+$: 533.1627; found 533.1627. $C_{22}H_{32}N_2O_9S_2$ (532.64): calcd C 49.61, H 6.06, N 5.26, S 12.04; found C 49.72, H 6.14, N 5.31, S 12.06.

*4.2.3. 4-Methylthiophenyl 2-acetamido-4-S-(2-acetamido-2-deoxy-β-D-glucopyranosyl)-2-deoxy-1,4-dithio-β-D-glucopyranoside (**3**)*

From **30** (45 mg, 0.05 mmol) in NaOMe/MeOH (10 mL). Colorless solid, yield: 28 mg (98%), mp 197.0–199.7 °C, R_f=0.53 ($CHCl_3$/MeOH, 7:3). $[\alpha]_D^{28}$ −67 (*c* 0.4, H_2O/50% DMSO). ^1H and ^{13}C NMR, see Tables 1 and 2. IR: ν=3281 (br ss), 2925 (s), 1654 (ss), 1562 (ss), 1407 (br s), 1374 (s), 1105 (s), 1057 (br s), 812 (w), 613 (m) cm^{-1}. HR ESI MS: $C_{23}H_{35}N_2O_9S_3$, calcd $[M+H]^+$: 579.1505; found 579.1514. $C_{23}H_{34}N_2O_9S_3$ (578.73): calcd C 47.74, H 5.92, N 4.84, S 16.62; found C 47.65, H 5.99, N 4.76, S 16.53.

*4.2.4. 4-Methylphenyl 2-acetamido-4-S-(2-acetamido-2-deoxy-β-D-glucopyranosyl)-2-deoxy-1,4-dithio-β-D-glucopyranoside (**4**)*

From **31** (62 mg, 0.11 mmol) in NaOMe/MeOH (10 mL). Colorless solid, yield: 57.1 mg (95%), mp 320 °C, R_f=0.51 ($CHCl_3$/MeOH, 7:3). $[\alpha]_D^{28}$ −16 (*c* 0.12, MeOH). ^1H and ^{13}C NMR, see Tables 1 and 2. IR:. ν=3277 (br s), 1652 (ss), 1545 (s), 1493 (m), 1373 (ss), 1314 (m), 1032 (br ss), 945 (s), 876 (m), 805 (m) cm^{-1}. HR ESI MS: $C_{23}H_{35}N_2O_9S_2$, calcd $[M+H]^+$: 547.1784; found 547.1773. $C_{23}H_{34}N_2O_9S_2$ (546.4), calcd C 50.54, H 6.27, N 5.12, S 11.73; found C 50.31, H 6.19, N 4.99, S 11.68.

*4.2.5. 4-Methoxyphenyl 2-acetamido-4-S-(2-acetamido-2-deoxy-β-D-glucopyranosyl)-2-deoxy-4-thio-β-D-glucopyranoside (**5**)*

From **32** (113 mg, 0.13 mmol) in NaOMe/MeOH (20 mL). Colorless solid, yield: 69 mg (98%), mp 240.3–241.0 °C, R_f=0.25 ($CHCl_3$/MeOH, 7:3). $[\alpha]_D^{23}$ −13 (*c* 0.2, H_2O). ^1H and ^{13}C NMR, see Tables 1 and 2. IR: ν=3347 (br ss), 2930 (m), 1658 (ss), 1548 (s), 1507 (ss), 1381 (s), 1219 (s), 1058 (br ss), 752 (m) cm^{-1}. HR ESI MS: $C_{23}H_{35}N_2O_{11}S$, calcd $[M+H]^+$: 547.1962; found 547.1967. $C_{23}H_{34}N_2O_{11}S$ (546.60): calcd C 50.54, H 6.27, N 5.13, S 5.87; found C 50.38, H 6.31, N 5.09, S 5.92.

*4.2.6. 2-Methyl 4-S-[(2-deoxy-2-thioacetamido-β-D-glucopyranosyl)]-(1,2-dideoxy-α-D-glucopyrano)-[2,1-d]-2-thiazoline (**6**)*

From **33** (70 mg, 0.09 mmol) in NaOMe/MeOH (20 mL). Colorless solid, yield: 39 mg (98%), mp 146.0–148.0 °C, R_f=0.55 ($CHCl_3$/MeOH, 7:3). $[\alpha]_D^{27}$ +25 (*c* 0.4, H_2O). ^1H and ^{13}C NMR, see Tables 1 and 2. IR: ν=3330 (br ss), 3059 (s), 2928 (s), 1621 (m), 1556 (m), 1385 (br s), 1277 (m), 1172 (s), 1051 (br ss) cm^{-1}. HR ESI MS: $C_{16}H_{27}N_2O_7S_3$, calcd $[M+H]^+$: 455.0980; found 455.0996. $C_{16}H_{26}N_2O_7S_3$ (454.59): calcd C 42.28, H 5.77, N 6.16, S 21.16; found C 42.02, H 5.95, N 5.98, S 21.32.

4.3. NMR spectroscopy

Spectra were recorded at ambient temperature in D_2O partly without sample spinning using the HDO signal as internal reference (4.70 ppm). Data acquisition was performed using X-WIN NMR 3.5 software, whereas processing was performed using the Topspin 1.3 software. For the assignment of the ^1H and ^{13}C signals a combination of ^1H and ^{13}C NMR spectroscopy, COSY, HMQC, HMBC, TOCSY, and NOESY (mixing times: 250, 500, and 800 ms) experiments with HDO suppression if necessary were recorded with a relaxation delay of 2 s. For the calculation of the rotameric population of gg-, gt-, and tg-conformers of the exocyclic hydroxymethyl group, additional J_{res} spectra were recorded; for the analysis the Eqs. I–III in Table 4 were employed.

4.4. Molecular modeling

Force field calculations were performed on a workstation, the ab initio calculations were performed on a PC-Linux cluster. The calculations were prepared and analyzed with the Sybyl 7.0 program package.[57] Force field calculations were run with a modified AMBER[58–60] force field implemented in the Sybyl 7.0 program package. The force field was expanded with additional GLYCAM04[61] parameters (based on GLYCAM93 parameterized by Woods et al. for carbohydrates[44]) and a new set of parameters developed to be constituent with AMBER. The new atom types and parameters for bond lengths, bond angles, torsional angles, improper torsions, and van der Waals parameters are shown in Tables S1–S6 in Supplementary data.

Most of the new parameters were achieved by the well established method by deducing from known similar parameters. Additionally, some torsional angles had to be determined by fitting the force field function on an ab initio grid search function (OS-CG-SS-CG, OS-CG-SS-CA, OS-CG-OS-CA) (see Supplementary data, S1–S3), which were calculated at the HF/6-31G* level of theory with the *opt=z-matrix* keyword and a systematic variation of the observed torsional angles in 10° increments from 0 to 350° as a scan calculation. On the other hand, the monomer database of the *biopolymer sugar dictionary* included in Sybyl had to be expanded to create compounds **1**–**6**. The new monomers were first of all geometry optimized with the *opt* keyword at the HF/6-31G* level of theory without restrictions using the Gaussian 03 suite of programs.[62] Afterward, HF/6-31G* single point calculations were run with the keyword *pop=mk iop*(6/33=2) to get electrostatic points in a form that the RESP program understands. RESP is a freely downloadable program, to assist and automatize the process of calculating RESP charges (prepared by A. Pigache, P. Cieplak, and F.-Y. Dupradeau). With these electrostatic points for every monomer, the 2-stage-restraint-multiple-conformation-ESP-charges (RESP charges) were assigned, that consider several conformations, and not only the low-energy conformations, as well as corresponding molecular symmetry[63,64] and added for every new monomer together with the *z*-matrix, the atom types and the connectivity information in the sybyl *biopolymer sugar dictionary*.

Two different calculations were considered with either *anti*- or *syn*-orientation for the H2–C2–NH torsion angle of the acetamide group. Additionally, the experimentally found ω and ω′ hydroxymethyl group orientations were used. Following, the force field grid search calculations of the oligosaccharides were run in 10°

increments from 0 to 350° and the local minima were relaxed afterward. 1,4-Interactions were scaled by a factor 0.5. A cut off the nonbonding interaction at 12 Å and a dielectric constant of 78 was used to implicitly consider the presence of water as solvent. The conformational plots were created with the OriginPro7.0 software. All calculations according to the *Boltzmann* function were done at 298 K.

Acknowledgements

This work was supported by the Deutsche Forschungsgemeinschaft (DFG) KL 754/8 (to E.K.) and Pe 264/18 (to M.G.P.). We thank Prof. K.-D. Spindler and Mr. Wagemann, University of Ulm, for enzyme assays and Prof. V.G.H. Eijsink for providing the *S. marcescens* chitinases.

Supplementary data

Force field parameterization data and experimental data of the precursor compounds **7**–**33** are available as Supplementary data free of charge via the Internet. Supplementary data in association with this article can be found in the online version at doi:10.1016/j.tet.2009.03.067.

References and notes

1. Semino, C. E.; Allende, M. L. *Int. J. Dev. Biol.* **2000**, *44*, 183.
2. van der Holst, P. P. G.; Schlaman, H. R. M.; Spaink, H. P. *Curr. Opin. Struct. Biol.* **2001**, *11*, 608.
3. Peter, M. G. *Biopolymers*; Wiley-VCH: Weinheim, 2002; p 481.
4. Ujita, M.; Sakai, K.; Hamazaki, K.; Yoneda, M.; Isomura, S.; Hara, A. *Biosci. Biotechnol. Biochem.* **2003**, *67*, 2402.
5. Rao, F. V.; Houston, D. R.; Boot, R. G.; Aerts, J.; Sakuda, S.; van Aalten, D. M. F. *J. Biol. Chem.* **2003**, *278*, 20110.
6. Fusetti, F.; von Moeller, H.; Houston, D.; Rozeboom, H. J.; Dijkstra, B. W.; Boot, R. G.; Aerts, J.; van Aalten, D. M. F. *J. Biol. Chem.* **2002**, *277*, 25537.
7. Vinetz, J. M.; Dave, S. K.; Specht, C. A.; Brameld, K. A.; Xu, B.; Hayward, R.; Fidock, D. A. *Proc. Natl. Acad. Sci. U.S.A.* **1999**, *96*, 14061.
8. Recklies, A. D.; White, C.; Ling, H. *Biochem. J.* **2002**, *365*, 119.
9. van Aalten, D. M. F.; Komander, D.; Synstad, B.; Gaseidnes, S.; Peter, M. G.; Eijsink, V. G. H. *Proc. Natl. Acad. Sci. U.S.A.* **2001**, *98*, 8979.
10. Germer, A.; Peter, M. G.; Kleinpeter, E. *J. Org. Chem.* **2002**, *67*, 6328.
11. Houston, D. R.; Shiomi, K.; Arai, N.; Omura, S.; Peter, M. G.; Turberg, A.; Synstad, B.; Eijsink, V. G. H.; van Aalten, D. M. F. *Proc. Natl. Acad. Sci. U.S.A.* **2002**, *99*, 9127.
12. Germer, A.; Klod, S.; Peter, M. G.; Kleinpeter, E. *J. Mol. Model.* **2002**, *8*, 231.
13. Germer, A.; Mügge, C.; Peter, M. G.; Rottmann, A.; Kleinpeter, E. *Chem.—Eur. J.* **2003**, *9*, 1964.
14. Eijsink, V. G. H.; Synstad, B.; Kolstad, G.; Gaseidnes, S.; Komander, D.; Houston, D.; Peter, M. G.; van Aalten, D. M. F. *Adv. Chitin Sci.* **2002**, *6*, 71.
15. Vaaje-Kolstad, G.; Houston, D. R.; Rao, F. V.; Peter, M. G.; Synstad, B.; van Aalten, D. M. F.; Eijsink, V. G. H. *Bioenergetics* **2004**, *1696*, 103.
16. Vaaje-Kolstad, G.; Vasella, A.; Peter, M. G.; Netter, C.; Houston, D. R.; Westereng, B.; Synstad, B.; Eijsink, V. G. H.; van Aalten, D. M. F. *J. Biol. Chem.* **2004**, *279*, 3612.
17. Cederkvist, F.; Zamfir, A. D.; Bahrke, S.; Eijsink, V. G. H.; Sorlie, M.; Peter-Katalinic, J.; Peter, M. G. *Angew. Chem., Int. Ed.* **2006**, *45*, 2429.
18. Thiele, G.; Rottmann, A.; Germer, A.; Kleinpeter, E.; Spindler, K. D.; Synstad, B.; Eijsink, V. G. H.; Peter, M. G. *J. Carbohydr. Chem.* **2002**, *21*, 471.
19. Wang, L. X.; Lee, Y. C. *J. Chem. Soc., Perkin Trans. 1* **1996**, 581.
20. Montero, E.; Garcia-Herrero, A.; Asensio, J. L.; Hirai, K.; Ogawa, S.; Santoyo-González, F.; Cañada, F. J.; Jiménez-Barbero, F. J. *Eur. J. Org. Chem.* **2000**, *10*, 1945.
21. Bock, K.; Duus, J. O.; Refn, S. *Carbohydr. Res.* **1994**, *253*, 51.
22. Aguilera, B.; Jiménez-Barbero, F. J.; Fernández-Mayoralas, A. *Carbohydr. Res.* **1998**, *308*, 19.
23. Raimbaud, E.; Buléon, A.; Pérez, S. *Carbohydr. Res.* **1992**, *227*, 351.
24. Tsai, C. S.; Reyes-Zamora, C.; Otson, R. *Biochim. Biophys. Acta* **1971**, *250*, 172.
25. Paul, B.; Korytnyk, W. *Carbohydr. Res.* **1984**, *126*, 27.
26. Barr, B. K.; Holewinski, R. J. *Biochemistry* **2002**, *41*, 4447.
27. Coutinho, P. M.; Henrissat, B. In *Recent Advances in Carbohydrate Bioengineering*; Gilbert, H. J., Davies, G., Henrissat, B., Svensson, B., Eds.; The Royal Society of Chemistry: Cambridge, 1999; p 3; See also: Carbohydrate Active Enzymes database (URL: http://www.cazy.org/).
28. Mark, B. L.; Vocadlo, D. J.; Knapp, S.; Triggs-Raine, B. L.; Withers, S. G.; James, M. N. G. *J. Biol. Chem.* **2001**, *276*, 10330.
29. Tews, I.; Perrakis, A.; Oppenheim, A.; Dauter, Z.; Wilson, K.; Vorgais, C. *Nat. Struct. Biol.* **1996**, *3*, 638.
30. Lillelund, V. H.; Jemnsen, H. H.; Liang, X.; Bols, M. *Chem. Rev.* **2002**, *102*, 515.
31. Terwisscha van Scheltinga, A. C.; Armand, S.; Kalk, K. H.; Isogai, A.; Henrissat, B.; Dijkstra, B. W. *Biochemistry* **1995**, *34*, 15619.
32. Tews, I.; Terwisscha van Scheltinga, A. C.; Perrakis, A.; Wilson, K. S.; Dijkstra, B. W. *J. Am. Chem. Soc.* **1997**, *119*, 7954.
33. Peters, T.; Pinto, B. *Curr. Opin. Struct. Biol.* **1996**, *6*, 710.
34. Cumming, D.; Carver, J. *Biochemistry* **1987**, *26*, 6664.
35. Tanaka, M.; Kyosaka, S.; Sekiguchi, Y. *Chem. Pharm. Bull.* **1976**, *24*, 3144.
36. Tanaka, M.; Kyosaka, S.; Ito, Y. *Chem. Pharm. Bull.* **1973**, *21*, 1971.
37. Micheel, F.; van de Kamp, F. P.; Petersen, H. *Chem. Ber.* **1957**, *90*, 521.
38. Horton, D.; Wolfrom, M. L. *J. Org. Chem.* **1962**, *27*, 1794.
39. Zemplén, G. *Ber. Dtsch. Chem. Ges.* **1927**, *60*, 1555.
40. Cava, M. P.; Levinson, M. I. *Tetrahedron* **1985**, *41*, 5061.
41. Jesberger, M.; Davis, T. P.; Barner, L. *Synthesis* **2003**, *13*, 1929.
42. Peikow, D. *Synthese und Glycosidasehemmung von Thio-analogen Kohlenhydraten PhD-thesis*; University of Potsdam, **2006**, URL: http://opus.kobv.de/ubp/volltexte/2006/1119/.
43. Gronenborn, A. M.; Clore, G. M. *Nucl. Magn. Reson. Spectrosc.* **1985**, *17*, 1.
44. Woods, R.; Dwek, R.; Edge, C.; Fraser-Reid, B. *J. Phys. Chem.* **1995**, *99*, 3832.
45. Atkins, P.; de Paula, J. *Physikalische Chemie*, 4th ed.; VCH: Weinheim, 2006.
46. Gerlt, J.; Youngblood, A. *J. Am. Chem. Soc.* **1980**, *102*, 7433.
47. Manor, P.; Saenger, W.; Davies, D.; Janowski, K.; Rabczenko, A. *Biochim. Biophys. Acta* **1974**, *340*, 472.
48. Wu, G.; Serianni, A.; Baker, R. *J. Org. Chem.* **1983**, *48*, 1750.
49. Nishida, Y.; Hori, H.; Ohuri, H.; Meguro, H. *J. Carbohydr. Chem.* **1988**, *7*, 239.
50. Nishida, Y.; Hori, H.; Ohuri, H.; Meguro, H. *Carbohydr. Res.* **1987**, *170*, 106.
51. Espionosa, J. F.; Asensio, J.; Bruix, M.; Jiménez-Barbero, F. J. *J. An. Quim.* **1996**, *92*, 320.
52. Muñoz, J. L.; Garcia-Herrero, A.; Asensio, J. L.; Auzennaeau, F. I.; Cañada, F. J.; Jiménez-Barbero, F. J. *J. Chem. Soc., Perkin Trans. 1* **2001**, 867.
53. Leeflang, B.; Vliegenhardt, J.; Kroon-Batenburg, L.; van Eijck, B.; Kroon, J. *Carbohydr. Res.* **1992**, *230*, 41.
54. Dowd, M.; French, A.; Reilly, P. *Carbohydr. Res.* **1992**, *233*, 15.
55. Engelsen, S.; Perez, S.; Braccini, I.; Herve du Pont, C. *J. Comput. Chem.* **1995**, *16*, 1096.
56. Mo, F. *Acta Chem. Scand.* **1979**, *A33*, 207.
57. SYBYL. *Molecular Modeling Software*; TRIPOS: St. Louis, MO, 2004.
58. Reiling, S.; Schlenkrich, M.; Brickmann, J. *J. Comput. Chem.* **1996**, *17*, 450.
59. Glennon, T.; Merz, K., Jr. *J. Mol. Struct.* **1997**, *395–396*, 157.
60. Cornell, W.; Cieplak, P.; Bayly, C.; Gould, I.; Merz, K.; Ferguson, D.; Spellmeyer, D.; Fox, T.; Caldwell, J.; Kollmann, P. *J. Am. Chem. Soc.* **1995**, *117*, 5179.
61. Glycam Parameters from http://glycam.ccrc.uga.edu/documents/gl_params.html.
62. Frisch, M. J.; Trucks, G. W.; Schlegel, H. B.; Scuseria, G. E.; Robb, M. A.; Cheeseman, J. R.; Montgomery, J. A., Jr.; Vreven, T.; Kudin, K. N.; Burant, J. C.; Millam, J. M.; Iyengar, S. S.; Tomasi, J.; Barone, V.; Mennucci, B.; Cossi, M.; Scalmani, G.; Rega, N.; Petersson, G. A.; Nakatsuji, H.; Hada, M.; Ehara, M.; Toyota, K.; Fukuda, R.; Hasegawa, J.; Ishida, M.; Nakajima, T.; Honda, Y.; Kitao, O.; Nakai, H.; Klene, M.; Li, X.; Knox, J. E.; Hratchian, H. P.; Cross, J. B.; Adamo, C.; Jaramillo, J.; Gomperts, R.; Stratmann, R. E.; Yazyev, O.; Austin, A. J.; Cammi, R.; Pomelli, C.; Ochterski, J. W.; Ayala, P. Y.; Morokuma, K.; Voth, G. A.; Salvador, P.; Dannenberg, J. J.; Zakrzewski, V. G.; Dapprich, S.; Daniels, A. D.; Strain, M. C.; Farkas, O.; Malick, D. K.; Rabuck, A. D.; Raghavachari, K.; Foresman, J. B.; Ortiz, J. V.; Cui, Q.; Baboul, A. G.; Clifford, S.; Cioslowski, J.; Stefanov, B. B.; Liu, G.; Liashenko, A.; Piskorz, P.; Komaromi, I.; Martin, R. L.; Fox, D. J.; Keith, T.; Al-Laham, M. A.; Peng, C. Y.; Nanayakkara, A.; Challacombe, M.; Gill, P. M. W.; Johnson, B.; Chen, W.; Wong, M. W.; Gonzalez, C.; Pople, J. A. *Gaussian 03, Revision B.03*; Gaussian: Pittsburgh, PA, 2003.
63. Bayly, C. I.; Cieplak, P.; Cornell, W. D.; Kollman, P. A. *J. Phys. Chem.* **1993**, *97*, 10269.
64. Cornell, W. D.; Cieplak, P.; Bayly, C. I.; Kollman, P. A. *J. Am. Chem. Soc.* **1993**, *115*, 9620.